and K is calculated from the bulk material. The pore content can be calculated by using Drude's equation [31] $(1-p)=(n_f^2-1)/(n_b^2-1)-1$. Results are summarized on Table 1. As observed, the proposed method produces dense films, compared with the bulk ZnO density (5.61 gcm^{-3},) with high pore content, probably due to the effect of the Triton X-100, since the production of CO_2 during the thermal decomposition of the xerogel it´s enhanced by the presence of this compound, which also contributes to the decrease of the refractive index (bulk= 1.9952). On the other hand, there isn´t appreciable difference from both Ag contents films.

Table 1. Physical properties of ZnO:Ag thin films.

Ag / mol %	Refractive index /u.a	Thickness / nm	Density / g cm^{-3}	Porosity / %
2.5	1.8695	595	5.12	15.5
5.0	1.8796	612	5.17	14.2

Optical transmittance spectra of Ag^+ 5 mol % thin film annealed at 500°C, in the wavelength range of 300 to 800 nm, is shown in Figure 2a. The film exhibit a transmittance higher than 80% within the visible region, which is ideally for its use in glass-windows, with a sharp fundamental absorption edge at 380 nm. The ZnO:Ag^+ film band gap was calculated according the Tauc model [32]:

$$\alpha h\nu \propto \left(h\nu - E_g\right)^{1/2}$$

Where hν is the photon energy, α is the absorption coefficient which could be derived from the transmittance data. Accordingly, the optical band gap can be obtained by extrapolating the corresponding straight lines downwards to the photon energy axis in a hν vs $(\alpha h\nu)^{1/2}$ plot (Figure 2b). The calculated band gap for the Ag^+ 5 mol % doped sample was 3.16 eV, which is in good agreement with the reported data for co-precipitation ZnO-powders of 3.17 eV [33], and which is lower the un-doped sample (3.20 eV).

Figure 2. a) Optical transmittance spectra b) Band gap estimation

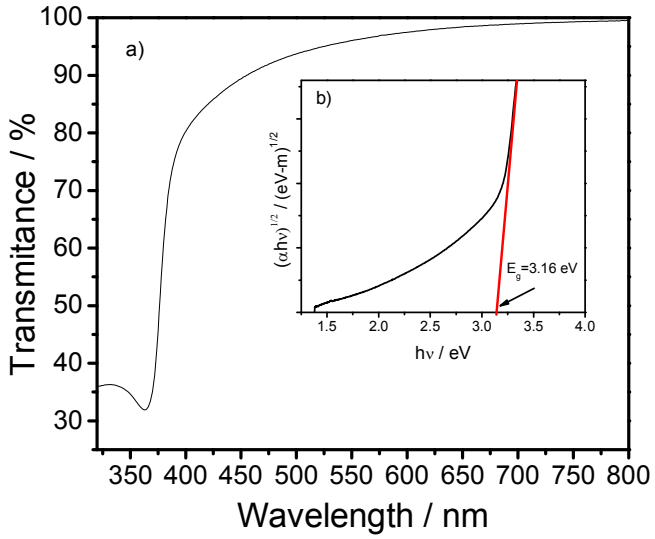

Figure 3 shows the XRD patterns for ZnO films doped at 2.5 and 5 mol %, and annealed at 500 °C. As observed, both samples had similar XRD patterns with high crystallinity, corresponding to the ZnO wurtzite hexagonal structure (space group C6mc) with lattice parameters a = 3.2496 Å and c = 5.2065 Å, according to JCPDS Card No. 36-1451. The calculated crystal sizes, calculated from the Scherrer's formula taking into account the line broadening of the diffracted peak due to the effect of crystal size, are 11.5 and 14.3 nm for the 2.5 and 5.0 mol % samples, respectively

Figure 3. XRD for Ag-doped ZnO sol-gel derived thin films as function of the Ag content, 500°C.

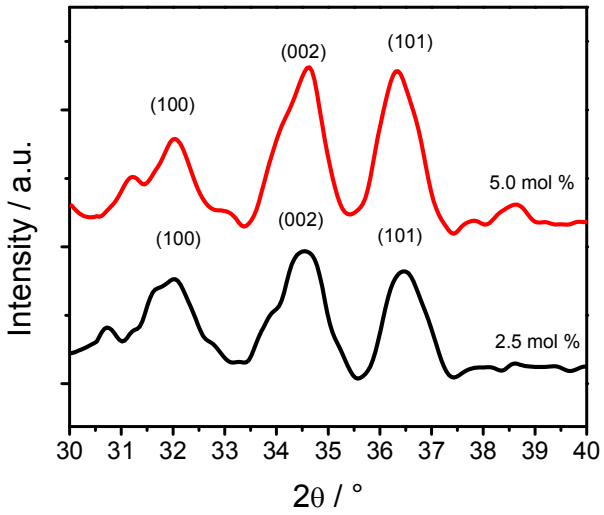

2.3. Morphological studies.

The morphology of the films was determined by means of SEM microscopy. Figure 4a presents a typical micrograph of the 5.0 mol % sample annealed at 500 °C, where can be observed that is almost crack-free, which it is particular important for the antibacterial materials, since physical homogeneity of the films avoid the presence bacterial colonies in the formed cracks. At higher magnifications, (Figure 4b) it can also observed the presences of some pores.

Figure 4. SEM micrographs of sol-gel derived ZnO:Ag^{+} films, a) 1000 X, b) 15,000 X.

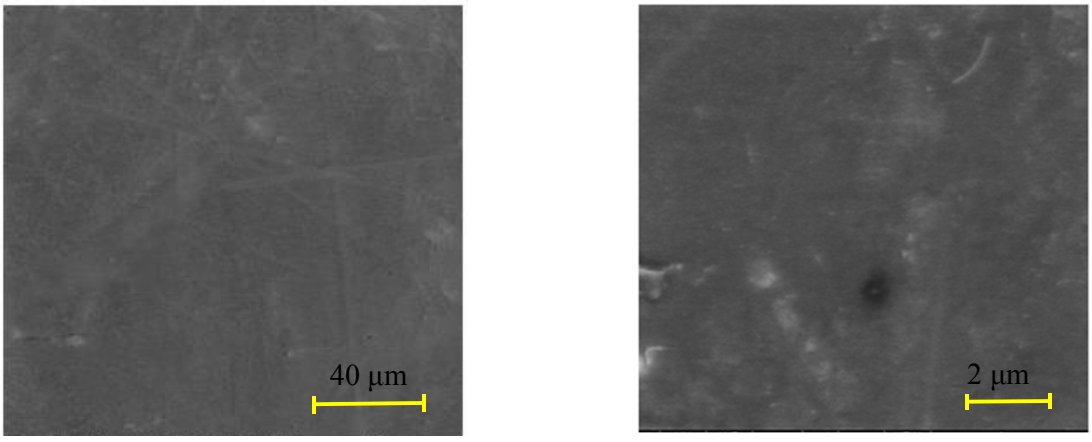

a) b)

The surface morphology sol-gel derived ZnO:Ag^+ films was evaluated by AFM. Figure 5a and b shows the micrograph 5.0 mol% sample annealed at 500 ℃ (2D and stereographic view, respectively). As can be observed, the films is constituted of close-packed fluffy nanoparticles dispersed all over the surface, with the presence of nanopores. The particle size measured is 20 ± 16 nm, and the surface of the films is very smooth, since the calculated roughness is 1.5 nm for the film.

Figure 5. AFM micrographs of sol-gel derived ZnO:Ag^+ films, a) 2D X, b) stereographic view.

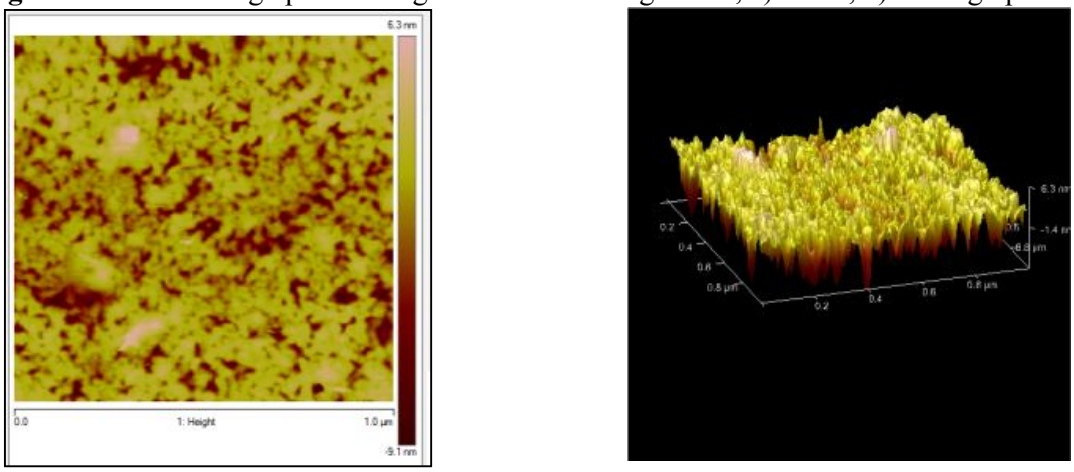

a) b)

2.4. Microbiological studies.

To evaluate the effect on *E. Coli* microbial growth over sol-gel derived ZnO:Ag^+ at different doping level (0-5 mol %), absorbance experiments were carried out in all systems to assess the net growth of cells, and the effect on the survival of the microorganisms over the films was evaluated by mean of CFU counting. Figure 6 shows the *E. Coli* CFU exposed to film as function of the Ag^+ content, and as observed, there is no significative antibacterial effect from the 2.5 sample, however, the antimicrobial ratio of the 5.0 sample reaches the 72 %, indicating that effectively the films presents antibacterial activity.

Figure 5. FCU/ 100 mL of *E.Coli* exposed to films as function of Ag^+ doping level.

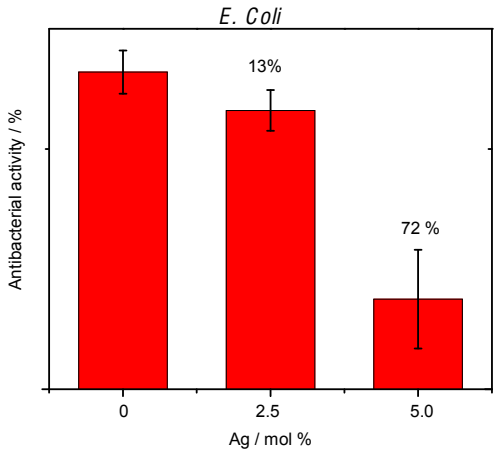

3. Experimental Section

The Ag-doped ZnO films on glass substrate were prepared by the sol-gel process and the dip-coating technique. First, Sol 1 was prepared as follows: a 1.13 M Zn sol was obtained dissolving zinc acetate dihydrate ($Zn(CH_3COO)_2 \cdot 2H2O$, Wako pure chemical industries, 99.0%), in iso-propanol ($CH3O_8H$, Alfa Aesar, 99%,) as solvent. A 50-50 Ethylene glycol-distilled water solution ($C_2H_6O_2$, Alfa Aesar, 99.0 %), were added in order to ensure the complete dissolution, and the sol is stirred vigorously for 3 h at 40 °C. Sol 2 was prepared as follows: a 0.043 M Ag sol was prepared dissolving silver acetate ($AgC_2H_3O_2$, Sigma-Aldrich, 99.0 %) in distilled water, and acetic acid (CH_3COOH, Alfa Aesar, 99.5 %) was added as a catalyst (4.3 M). The sol was stirred vigorously for 1 h at 60ºC to obtain a transparent sol. Later, both sols, Sol 1 and Sol 2, were mixed together in order to obtain a 2.5 or 5.0 Ag^+ mol % product, and subsequently Triton X-100 ($C_{14}H_{22}O(C_2H_4O)n$, Alfa Aesar, 99.0 %) was slowly incorporated into the sol under vigorous stirring at 50 °C, with Zn/Triton molar ratio of 15.0 (Triton X-100 average molecular weight=625 $gmol^{-1}$). The final sol was transparent and stable for 12 h. For the deposition of film, the substrates (Corning glass) were first carefully degreased and cleaned before deposition, and later dipped into the prepared sol and pulled up at a constant rate of 4.0 cm s^{-1}. Subsequently, to remove the water content and the most volatile organic compounds, dipped substrates were dried for 10 min at 100 °C. The procedure of coating and drying was repeated for three times. Finally, for the ZnO formation, the films were set on a furnace at 500 °C for one hour. The final appearance of the transparent films is showed on Figure 7.

Figure 7. Photograph of transparent Ag-doped ZnO Triton X100 modified film at 500°C.

The behavior of the sol during the heat treatment was analyzed by means of IR spectra recorded in the 4000-450 cm^{-1} range using Fourier transform infrared spectroscopy (FTIR 2000, Perkin Elmer). Crystal structure was determined by X-Ray diffractometry (D8 Advance, Bruker AXS) using a Cu-Kλ radiation at 35 kV, 25 mA. Morphology was investigated by means of SEM microscopy in a Philips XL-30 operated at 5 kV). Surface morphology was analyzed by Nanoscope IV Atomic Force Microscopy with (Digital Instruments) in tapping mode. The thickness, refractive index, density and porosity were measured by m-lines spectroscopy, which uses a prism coupling method to launch a laser light into the optical layer. The prism (LaSF35, angle 60°) was coupled with a light of He-Ne laser with a wavelength λ equal to 633 nm into the waveguide.

To evaluate the effect on bacterial growth due to the exposition of the sol-gel derived ZnO:Ag films, *E. Coli* microorganisms obtained by a wastewater sample was used, and was cultured aerobically in brilliant green medium, at 37 °C on a rotary shaker (120 rpm) during 8 h, and maintained in Eosin Methylen Blue (EMB) agar plates (Becton Dickinson), at the same temperature overnight. Later, 50 mL of brilliant green broth was added in a 250 mL Erlenmeyer flask, and posteriorly was inoculated directly using a bacteriological loop from EMB agar plates. The obtained cultures were maintained at 37 °C overnight. Finally, 1 mL from the previous inoculate system was added to another Erlenmeyer flask with fresh medium in order to complete the antibacterial activity study. The effect on growth *E. Coli* on films was evaluated through the exposure of 1 cm^2 of the ZnO, surfaces doped with different silver content (0, 2.5 and 5 mol %), with 50 mL of brilliant green medium (Bile Broth 2%, Becton Dickinson) in an Erlenmeyer flasks of 250 mL capacity. The absorbance was measured along the microbial kinetics and at the end of exponential phase, and the Colony-forming unit (FCU) was quantified in EMB agar plates. All experiments were carried out by triplicate.

4. Conclusions

The present work synthetized ZnO:Ag Triton X-100 modified thin films by a sol-gel process. The films present high transparency, as well as a band gap lower than the bulk ZnO (3.20 to 3.15 eV for a 5.0 mol % Ag sample). The films shows a hexagonal wurtzite structure from 500 °C, and, as it was observed in FTIR measurements that almost all the organic compounds are eliminated at this temperature. The morphology of the films are homogeneous and almost crack-free, with the presence of residual pores probably product of the decomposition of the organic compounds during the annealing process. Finally, the antibacterial studies shown that for *E. Coli* bacteria, the higher microbicide effect is observed for the higher (5 mol %) Ag^+ doped sample, 72 % compared with 13 % at the lower sample (2.5 mol %).

Acknowledgments

The authors gratefully acknowledge the financial support of SEP-CONACYT 136219 and SIP 20131270 projects. Also wants to acknowledge the assistance of Eng. Oscar Francisco Rivera Dominguez for its contribution to the project.

Conflicts of Interest

The authors declare no conflict of interest.

References and Notes

1 Wang, G.; Zreiqat, H. Functional Coatings or Films for Hard-Tissue Applications. Materials **2010**, 3, 3994-4050.

2 Brayner,R.; Ferrari-Iliou, R.; Brivois,N.; Djediat, S.; Benedetti, M.F.; Fiévet, F. Toxicological Impact Studies Based on Escherichia coli Bacteria in Ultrafine ZnO Nanoparticles Colloidal Medium. Nano Letters **2006,** 6, 866-870.

3 Tam, K.H.; Djurišić, A.B.; Chan, C.M.N.; Xi, Y.Y.; Tse, C.W.; Leung, Y.H.; Chan, W.K.; Leung, F.C.C.; Au, D.W.T. Antibacterial activity of ZnO nanorods prepared by a hydrothermal method. Thin Solid Films **2008**, 516, 6167-6174.
4 P.J.A. Borm, W. Kreyling, J. Nanosci. Nanotechnol. 4 (2004) 521
5 Mungkalasiri, J.; Bedel, L.; Emieux, F.; Doré, J.; Renaud, F.N.R.; Sarantopoulos, C.; Maury, F. CVD Elaboration of Nanostructured TiO_2-Ag Thin Films with Efficient Antibacterial Properties. Chemical Vapor Deposition **2010,** 16, 35–41.
6 Yu, B.; Leung, K.M.; Guo, Q.; Lau, W.M.; Yang, J. Synthesis of Ag–TiO_2 composite nano thin film for antimicrobial application Nanotechnology **2011,** 22, 115603 (9p).
7 Mungkalasiri, J.; Bedel, L.; Emieux, F.; Vettese-Di Cara, A.; Freney, J.; Maury, F.; Renaud, F.N.R. Antibacterial properties of TiO_2–Cu composite thin films grown by a one-step DLICVD process. Surface and Coatings Technology **2014,** 242, 187-194.
8 Tseng, Y.H.; Sun D.S.; Wu W.S.; Chan H.; Syue M.S.; Ho H.C.; Chang H.H. Antibacterial performance of nanoscaled visible-light responsive platinum-containing titania photocatalyst in vitro and in vivo. Biochimia Biophysics Acta **2013,** 1830, 3787-3795.
9 Azizi, S.; Ahmad, M.B.H.; Hussein, M.Z.; Ibrahim, N.A. Synthesis, Antibacterial and Thermal Studies of Cellulose Nanocrystal Stabilized ZnO-Ag Heterostructure Nanoparticles. Molecules **2013**, 18, 6269-6280.
10 Jones, N.; Ray, B.; Ranjit, K.T.; Manna, A.C. Antibacterial activity of ZnO nanoparticle suspensions on a broad spectrum of microorganisms. FEMS Microbiology Letters **2008,** 279, 71–76.
11 Lin, L.Y.; Jeong, M.C.; Kim, D.E.; Myoung, J.M. Micro/nanomechanical properties of aluminum-doped zinc oxide films prepared by radio frequency magnetron sputtering. Surface and Coatings Technology **2006,** 201, 2547-2552.
12 Fang. T.H.; Jian, SR.; Chuu, D.S. Nanotribology and fractal analysis of ZnO thin films using scanning probe microscopy. Journal of Physics D: Applied Physics **2003**, 36, 878-883.
13 Thongsuriwong, K.; Amornpitoksuk, P.; Suwanboon, S. Structure, morphology, photocatalytic and antibacterial activities of ZnO thin film prepared by sol–gel dip-coating method. Advanced Powder Technology **2013,** 24, 275-280.
14 Padmavathy, N.; Vijayaraghavan, R. Enhanced bioactivity of ZnO nanoparticles–and antimicrobial study. Science and Technology of Advanced Materials **2008,** 9, 035004 (7p).
15 Hsiao, C.C.; Huang, K.Y.; Hu, Y.C. Fabrication of a ZnO Pyroelectric Sensor. Sensors **2008**, 8, 185-192.
16 Xu, P.; Zhuang, H. Fabrication and characterisation of multipod ZnO nanostructures by CVD on Al_2O_3-coat Si (111) substrate. Micro & Nano Letters **2011,** 6, 985-988.
17 Chakrabarti, S.; Doggett, B.; O'Haire, R.; McGlynn, E.; Henry, M.; Meaney, A.; Mosnier, J.P. Characterization of nitrogen-doped ZnO thin films grown by plasma-assisted pulsed laser deposition on sapphire substrates. Superlattices and Microstructures **2007,** 42, 21-25.
18 Lehraki, N.; Aida, M.S.; Abed, S.; Attaf, N. ZnO thin films deposition by spray pyrolysis: Influence of precursor solution properties. Current Applied Physics **2012**, 12, 1283–1287.
19 Scarel, G.; Na, J.S.; Gong, B.; Parsons, G.N. Phonon response in the infrared region to thickness of oxide films formed by atomic layer deposition. Applied Spectroscopy **2010,** 64 120-126.
20 Kathalingam, A.; Ambika, N.; Kim, M.R.; Elanchezhiyan, J.; Chae, Y.S.; Rhee, J.K. Chemical bath deposition and characterization of nanocrystalline ZnO thin films. Materials Science-Poland **2010,** 28, 513-522.
21 Márquez, J.A.R.; Herrera, C.M.; Fuentes, M.L.; Rosas, L.M. Effect of three operating variables on degradation of methylene blue by ZnO electrodeposited: Response surface methodology, International Journal of Electrochemical Science **2012,** 7, 11043-11051.
22 Mackenzie, J.D.; Bescher, E.P. Physical Properties of Sol-Gel Coatings. Journal of Sol-Gel Science and Technology **2000,** 19, 23-29.

23 Znaidi, L. Sol–gel-deposited ZnO thin films: A review, Materials Science and Engineering B **2010**, 174, 18–30.
24 Kozuja, H. Stress evolution on gel-to-ceramic thin film conversion. Journal of Sol-Gel Science and Technology **2006,** 40, 287-297.
25 Du, T.; Song, H.; Ilegbusi, O.J. Sol–gel derived ZnO/PVP nanocomposite thin film for superoxide radical sensor. Materials Science and Engineering: C **2007**, 27, 414-420.
26 Guo. H.; Tao, S. Sol-Gel Synthesis of Palladium-Doped Silica Nanocomposite Fiber Using Triton X-100 Micelle Template and the Application for Hydrogen Gas Sensing. IEEE Sensors Journal **2007**, 7, 323-328.
27 Kluson, P.; Kacer, P.; Cajthaml, T.; Kalaji, M. Preparation of titania mesoporous materials using a surfactant-mediated sol–gel method, Journal of Materials Chemistry **2001**, 11, 644-651.
28 Israr, M.Q.; Sadaf, J.R.; Nur, O.; Willander, M.; Salman, S.; Danielsson, B. Chemically fashioned ZnO nanowalls and their potential application for potentiometric cholesterol biosensor. Applied Physics Letters **2011**, 98, 253705 (3p).
29 Vafae, M.; Ghamsari, M.S. Preparation and characterization of ZnO nanoparticles by a novel sol–gel route. Materials Letters **2007**, 61, 265-3268.
30 Brusentsev, F. A.; Rebenko, N. Algol-60 program for calculating sin θ/λ values and the polarization- Lorentz factors LP. Structural Chemistry **1966**, 8, 406-413
31 Tien, P.K.; Ulrich, R. Theory of prism-film coupler and thin-film light guides. Journal of Optical Society of America **1970**, 60, 1325-1337.
32 Tauc J,; Grigorovici R,; Vancu A. Optical properties and electronic structure of amorphous germanium. Physica Status Solidi **1966**, 15, 627-637.
33 Sankara, R.B.; Venkatramana, R.S.; Koteeswara, R.N.; Pramoda, K.J. Synthesis, Structural, Optical Properties and Antibacterial activity of co-doped (Ag, Co) ZnO Nanoparticle. Research Journal of Material Sciences **2013,** 1, 11-20.